

# A Novel Automatic Extraction Method of Lung Texture Tree from HRCT Images

LIU Jun-Wei<sup>1</sup> FENG Huan-Qing<sup>1</sup> ZHOU Ying-Yue<sup>1</sup> LI Chuan-Fu<sup>1,2</sup>

**Abstract** Computed tomography (CT) is the primary imaging modality for investigation of lung function and lung diseases. High resolution CT slice images of chest contain lots of texture information, which provides powerful datasets to research computer aid-diagnosis (CAD) system. But the extraction of lung tissue textures is a challenge task. In this paper, we introduce a novel method based on level set to extract lung tissue texture tree, which is automatic and effectual. Firstly, we propose an improved implicit active contour model driven by local binary fitting energy, and the parameters are dynamic and modulated by image gradient information. Secondly, a new technique of painting background based on intensity nonlinear mapping is brought forward to remove the influence of background during the evolution of single level set function. At last, a number of contrast experiments are performed, and the results of 3D surface reconstruction show our method is efficient and powerful for the segmentation of fine lung tree texture structures.

**Key words** Active contour model, level set, local binary fitting energy, dynamic parameter modulation, 3D surface reconstruction

In recent years, active contour model has been widely used for image segmentation in computer vision. Active contour model (firstly proposed by Kass<sup>[1]</sup>) utilizes high phase human vision information of image by evolving closed contour. But it suffers several drawbacks, and the chief one is that it can not handle the topological changes of evolving contour so that multi-object images cannot be partitioned easily. Level set method for front propagation is a powerful means to handle topological changes, and it also removes the issues of contour parameterization and control point regriding<sup>[2]</sup>. Level set method was firstly introduced into active contour model by Caselles<sup>[3]</sup> and Malladi<sup>[4]</sup> independently, which was named as geometric active contours. These models fuse level set method and curve evolution theory together. Recently, a large number of image segmentation methods based on level set have been proposed. According to the model driven information of curve evolution, the existing methods can be cursorily classified into two categories — edge-based model<sup>[5–6]</sup> and region-based model<sup>[7–8]</sup>. Edge-based model generally contains two terms: an edge detection term and a driven force term. The edge-based model utilizes the grads of image and has complicated parameter setting, which may make the model not capable of partitioning the images with weak boundary object or thin tubular object. Region-based model, such as MumfordShah model<sup>[7]</sup> and active contours without edges (C-V model)<sup>[8]</sup>, uses global region information of images. The region-based model without grads information can treat images with weak boundary object. Moreover, it is less sensitive to the initial contours and gets more applicability. However, it can hardly segment the intensity inhomogeneity images. As a progressive development, a novel implicit active contours driven by local binary fitting (LBF) energy model was proposed by Li<sup>[9]</sup>. The LBF model is based on local region information of images and able to segment images with weak object boundaries, vessel-like structures, and intensity inhomogeneity.

Computed tomography (CT) is the primary imaging modality for investigation of lung function and lung diseases. It can provide high resolution computed tomogra-

phy (HRCT) serial images, which reveal the details of lung structure for clinician. Thoracic HRCT images contain lots of information about lung textures, which include trachea tree, lung vein tree, lung artery tree, and pathological tissues likely existing in lungs. Therefore, they are very important for lung disease diagnoses and researches of correlative computer aid-diagnosis (CAD) system. The existing automatic lung segmentation methods mainly eliminate the bones, the other tissues outside lungs, the trachea, and the main bronchia in thoracic CT images. However, the segmented lung region contains lots of lung textures. If they are used in diagnoses, wrong results always occur. There are two main reasons. First, the pathological structures in lung are very blurry because the segmented regions contain lots of lung textures. So, errors and misses will increase in diagnoses. Second, the abundant information in lung textures is very useful to analyze and orientate diseases. However, it is very difficult to segment lung textures clearly because of the structure complexity. During segmentation, the results are easily influenced by the partial volume effect.

Some articles have reported the segmentation of lung trachea and blood vessel. The frame of vessel segmentation is gradually formed<sup>[10]</sup>. However, these methods aim at the tubular structure and need set parameters alternately and find the positions of seed points<sup>[11–13]</sup>. So, a novel automatic segmentation method of lung texture tree based on level set is developed in this paper. The method does not need complex parameters and can extract all the lung textures in only one step of segmentation. The result of 3D surface reconstruction of segmented lung textures shows a good isotropy and integrality of segmentation.

## 1 Method

### 1.1 LBF model

The LBF model<sup>[9]</sup> is based on a mild assumption: the image can be approximated locally by a binary image. Let arbitrary grid point  $x$  belong to image domain  $\Omega: \Omega \rightarrow \mathbf{R}$ , and  $C$  be a contour in image  $I(x)$  represented by the zero level set of a Lipschitz function  $u(x): u(x) \subset \Omega$ . The total energy of LBF model, with respect to  $u(x)$ , is defined by

$$E(u, f_1, f_2) = \alpha L(u) + \beta D(u) + \int_{\Omega} E_{LBF}(x) dx \quad (1)$$

where  $\alpha$  and  $\beta$  are nonnegative constants,  $L(u)$  is the length term of the zero level set of  $u$ ,  $D(u)$  is a distance penalizing

Received January 9, 2008; in revised form April 8, 2008  
Supported by National Natural Science Foundation of China (60771007) and Natural Science Foundation of Anhui Education Department (2006KJ097A)

1. Department of Electronic Science and Technology, University of Science and Technology of China, Hefei 230027, P. R. China  
2. Medical Image Center, the First Affiliated Hospital, Anhui Traditional Medicine College, Hefei 230031, P. R. China

DOI: 10.3724/SP.J.1004.2009.00345

term to ensure stable evolution of level set function without re-initialization<sup>[6]</sup>, and  $E_{LBF}(x)$  is local binary fitting energy defined in [9]. To minimize the total LBF energy function, the gradient descent flow is expressed as

$$\frac{\partial u}{\partial t} = -\sigma(u)(g_1 e_1 - g_2 e_2) + \alpha \delta(u) \operatorname{div} \left( \frac{\nabla u}{|\nabla u|} \right) + \beta \left( \nabla^2 u - \operatorname{div} \left( \frac{\nabla u}{|\nabla u|} \right) \right) \quad (2)$$

where

$$e_1(x) = \int_{\Omega} K_{\sigma}(y-x) |I(x) - f_1(y)|^2 dy \quad (3)$$

$$e_2(x) = \int_{\Omega} K_{\sigma}(y-x) |I(x) - f_2(y)|^2 dy \quad (4)$$

$$f_1(x) = \frac{K_{\sigma}(x) * [H(u(x))I(x)]}{K_{\sigma}(x) * H(u(x))} \quad (5)$$

$$f_2(x) = \frac{K_{\sigma}(x) * [(1-H(u(x)))I(x)]}{K_{\sigma}(x) * [1-H(u(x))]} \quad (6)$$

$K_{\sigma}(x)$  is the Gaussian kernel function with variance  $\sigma$ , and  $\sigma(x)$  is Dirac function

$$\sigma(x) = \frac{1}{\pi} \frac{\epsilon}{\epsilon^2 + x^2} \quad (7)$$

Heviside function  $H(x)$  is defined by

$$H(x) = \frac{1}{2} \left[ 1 + \frac{2}{\pi} \arctan \left( \frac{x}{\epsilon} \right) \right] \quad (8)$$

In fact, for each point  $x$  on contour  $C$ , local binary fitting energy  $E_{LBF}(x)$  is defined as<sup>[9]</sup>

$$E_{LBF}(x) = g_1 \int_{in(C)} K_{\sigma}(x-y) |I(y) - f_1(x)|^2 dy + g_2 \int_{out(C)} K_{\sigma}(x-y) |I(y) - f_2(x)|^2 dy \quad (9)$$

When point  $x$  is exactly on the object contour, LBF energy  $E_{LBF}(x)$  achieves a minimization value. Otherwise, curve  $C$  is evolved by the two fitting values  $f_1(x)$  and  $f_2(x)$ , until all points of  $C$  are exactly on the contours of the object. Based on local information of images, LBF model can get accurate object boundaries by optimizing global LBF energy. Compared with other models, the model shows many advantages. It is able to partition MRI images with intensity inhomogeneity, which cannot be segmented accurately by region-based model. It also can partition images with weak boundary object or vessel-like object, which cannot be easily segmented by edge-based model. But the setting of LBF model parameters (such as  $\alpha, \beta, g_1$ , and  $g_2$ ) is an annoying work in application. There are huge differences between parameter settings for different images. In this paper, a dynamic parameter modulation method is introduced to conquer the drawback according to grad information of image.

## 1.2 Dynamic parameter LBF model (DPLBF)

$\alpha$  and  $\beta$  are enacted as positive constants, and region term parameters  $g(x)$  ( $g_1$  and  $g_2$  have the same formula) are variable. Dynamic parameter function  $g(x)$  is defined as

$$g(x) = A + \frac{B}{1 + \frac{C|\nabla(G * I(x))|^2}{\max(|\nabla(G * I(x))|^2)}} \quad (10)$$

where  $A$  is the basic part of  $g(x)$ ,  $B$  and  $C$  are dynamic modulation parameters,  $G(x)$  is the Gaussian kernel function, and  $\max(x)$  is the maximized value of  $x$ . Function  $g(x)$  gains a higher value, where there is lower image grads. Big region term parameters can promote evolution speed of curve. Otherwise, function  $g(x)$  gains a lower value at the point of image with higher grads, where it may be the contour of object. So curve evolution can be balanced by appropriate parameters of the LBF model. Moreover, length term acts mainly because of lower values of  $g(x)$ , and thereby illusory contours are avoided. After making improvement, the partial differential equation of DPLBF is defined by

$$\frac{\partial u}{\partial t} = -\sigma(u)(g_1(x)e_1 - g_2(x)e_2) + \alpha \delta(u) \operatorname{div} \left( \frac{\nabla u}{|\nabla u|} \right) + \beta \left( \nabla^2 u - \operatorname{div} \left( \frac{\nabla u}{|\nabla u|} \right) \right) \quad (11)$$

Finite difference method is used commonly for discretization of partial differential equation (PDE). After  $n$ -step iterations, the first order derivative of level set function  $u(x, t)$  can be approximately computed by one-sided finite difference as follows

$$\frac{\partial u(x, t)}{\partial t} \approx \frac{u_{n+1}(x) - u_n(x)}{\Delta t} \quad (12)$$

By Taylor expansion,  $n$  step level set function can be rewritten as

$$u_{n+1}(x) = u_n(x) + \frac{\partial u(x, t)}{\partial t} \frac{\Delta t}{1!} + \frac{\partial^2 u(x, t)}{\partial t^2} \frac{\Delta t^2}{2!} + \dots \quad (13)$$

Then, truncation error of the first order derivative can be computed as

$$\tau_{x,n} = \frac{u_{n+1}(x) - u_n(x)}{\Delta t} - \frac{\partial u(x, t)}{\partial t} = O(\Delta t) \quad (14)$$

Truncation error  $\tau_{x,n}$  has the same order as  $\Delta t$ . As we generally select an exactly small  $\Delta t$ , difference formula  $\frac{u_{n+1}(x) - u_n(x)}{\Delta t}$  is nearly equal to  $\frac{\partial u(x, t)}{\partial t}$ . But in some occasions, truncation error  $\tau_{x,n}$  could be very large, when level set function  $u(x, t)$  changes acutely. Large truncation error can badly reduce the accurateness of lung texture extraction. Centered finite difference of the first order derivative can be defined as

$$\frac{u_{n+1}(x) - u_{n-1}(x)}{2\Delta t} = \frac{\partial u(x, t)}{\partial t} + O(\Delta t^2) \quad (15)$$

At this time, truncation error  $\tau_{x,n}$  obviously has the same order as  $O(\Delta t^2)$ . Centered difference has a much smaller truncation error than one-sided difference. Then, we can gain the following leapfrog finite difference formula of PDE of DPLBF model

$$u_{n+1}(x) = u_{n-1}(x) + 2\Delta t F(u_n(x)) \quad (16)$$

where function  $F(u_n(x))$  is the centered difference formula of right side of (11). The truncation errors of time domain and space domain are much smaller, which make the evolving level set function accurate and stable.

## 2 Image preprocessing

### 2.1 Lung region extraction

Structure continuity is a marked characteristic of high resolution CT serial images. It means that the changes between two adjacent slices are successive. In order to make full use of the characteristic, a segmentation strategy based on the structure continuity is employed. Primitively, a slice is chosen as the template image from the thoracic HRCT series. We segment the template and get the lung mask. Then, we segment new images in two directions slice by slice. One direction is from the template to lung apex, and the other is from the template to lung base. The lung mask about new image is restricted by the previous lung mask. When we segment a thoracic slice, the threshold and morphologic methods are used to get the coarse lung images. Let  $M$  be the current slice. First, we get the mask of the body region  $Mb = Bwselect[(M \geq T_1) \times SE_1]$ .  $T_1$  is  $-200$  HU, which is the lower threshold about other tissue except lung in the thorax. The structure element  $SE_1$  is used to close the holes in the body region.  $Bwselect$  represents the operation of selecting the object in morphologic method. The origin point of  $Bwselect$  is the center of  $M$ . Second, we segment the lung region  $Mc = Mb \times M \geq T_2 \times Mb$ .  $T_2$  is  $-500$  HU, which is the upper threshold about lung. Third, we modify  $Mc$  to get lung mask  $Mask = Mc \times SE_2$ . The structure element  $SE_2$  is used to close the small holes and cracks in the lung region. At last, we get the lung image  $LungRegion = Mask \times M$ . In segmented results, there may be some cracks and indentations in lung edges, where vessels come into lung. Vessels have higher values than other lung tissues, so they could be removed unconsciously. A rolling ball technique can be used to remedy the cracks and indentations by making an opening operation<sup>[14]</sup>. Fig. 1 shows the result of lung region extraction.

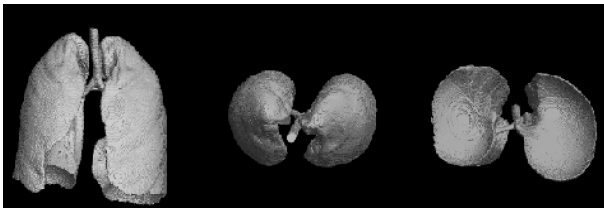


Fig. 1 3D surface recognition of lung tissue region (The images from left to right are the results of 3D surface-rendered lung in the coronary, top-to-base, and base-to-top view.)

### 2.2 Technique of painting background

Technique of painting background is derived from human vision system theory. Simultaneous brightness contrast research by Heinemann<sup>[15]</sup> indicates that object recognition of human vision depends on not only the self-saliency features of object but also the relative saliency features between object and background. Therefore, internal details of object can be enhanced by reducing the contrast between object and its background. C-V model has been used in detecting internal contours of object in the observed image by changing the background in image<sup>[16]</sup>. Technique of painting background with a linear intensity transformation is effective for C-V model based on global region information, while it is of no effect for DPLBF model based on local region information. So, nonlinear intensity transformation is brought in urgently.

Nonlinear intensity transformation is designed to enhance the intensities of certain range, by which image information is convenient for computer processing. Let  $\mu$  be intensity of pixel before transformation and  $\nu$  be transformed intensity. In this paper, a nonlinear intensity transformation formula is defined by

$$\nu = I_{\min} + \frac{I_{\max} - I_{\min}}{1 + e^{-\frac{\mu}{I_{\text{mean}}}}} \quad (17)$$

where  $I_{\max}$  is the maximized intensity,  $I_{\min}$  is the minimized intensity, and  $I_{\text{mean}}$  is the mean intensity of object image region. In Fig. 2, certain range intensity is compressed or extended selectively: 1) Region A with a higher intensity possibly contains intensity of lung texture tree. The intensities of A are compressed more closely and constrictively. Thereby, intensity of lung texture tree achieves region coherence and is favorable to be segmented. 2) Intensities of background and remaining region B are extended to an extreme from region A. So, the influence of background is potentially wiped off during the extraction of lung texture tree.

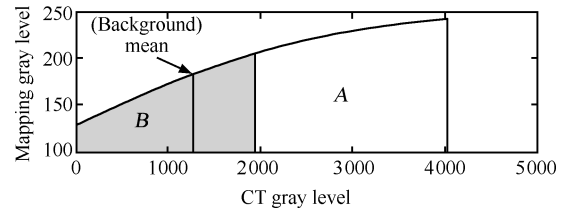


Fig. 2 Nonlinear intensity transformation curve

## 3 Results of experiments

### 3.1 Improvement of dynamic parameter modulation

LBF model can segment the manual image with intensity inhomogeneity in Fig. 3, while C-V model cannot segment it accurately<sup>[9]</sup>. We select fixed region term parameters and penalizing term parameters of LBF and DPLBF. By changing the length term parameters, we show the advantages of DPLBF. Let  $g_1 = g_2 = 2$  and  $\beta = 1$  in LBF model. In relative range, let  $A_1 = A_2 = 1$ ,  $B_1 = B_2 = 2$ ,  $C_1 = C_2 = 1$ , and  $\beta = 1$  in DPLBF model. Let  $\alpha = a \times 255 \times 255$  in LBF and DPLBF jointly. From contrast experiments in Fig. 3, we can draw two conclusions: 1) when parameter  $a$  is between 0.01 and 0.05, both models can segment the image accurately. But at  $a = 0.055$ , LBF achieves local optimization, while DPLBF is effective; when LBF is of no effect at  $a = 0.09$ , DPLBF is still able to segment image accurately. 2) DPLBF has a larger region-driven force, where grads of image is smaller. Thereby, speed of curve evolution is fast and parameters are easily set using dynamic parameter modulation method, which makes LBF model more applicable.

### 3.2 Segmentation of lung CT slice image

We compare experimental results of each method in Fig. 4. The result of region-based model (C-V model) is piecewise and broken up without concerning local information. The result of edge-based model is locally optimized and cannot deal with thin texture structures. The result of DPLBF using intensity linear transformation has many illusive contours. The method proposed in this paper can extract thin texture structures accurately and exquisitely.

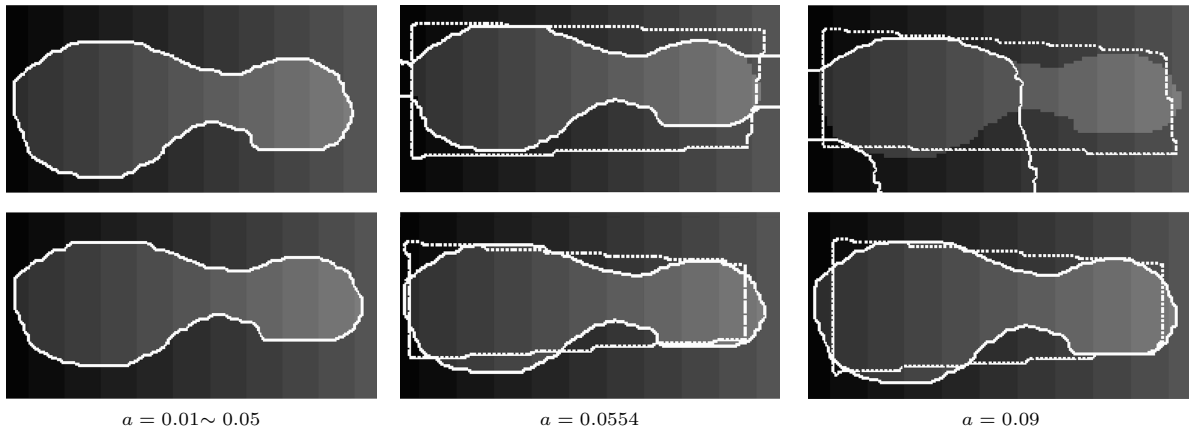
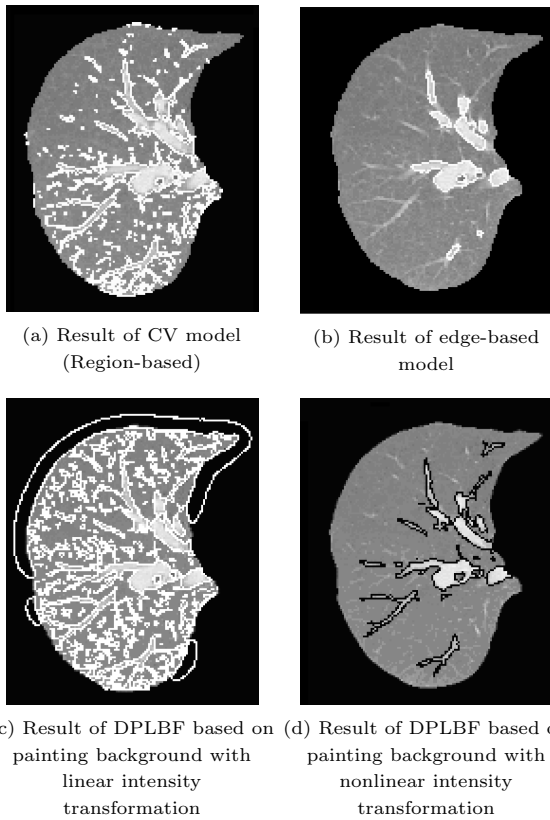


Fig. 3 Improved results of dynamic parameter modulation (The first row are the results of LBF model and the second row are the results of DPLBF model.)



(a) Result of CV model (Region-based)

(b) Result of edge-based model

(c) Result of DPLBF based on painting background with linear intensity transformation

(d) Result of DPLBF based on painting background with nonlinear intensity transformation

Fig. 4 Comparing results of three category models

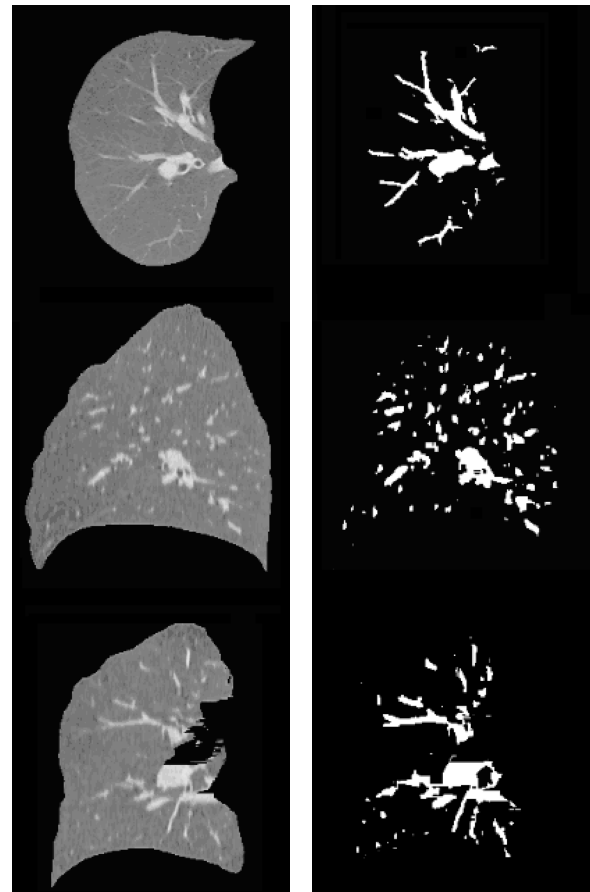
### 3.3 Texture extraction of 3D database

We select a 3D HRCT database with size of  $512 \times 512 \times 297$  pixels. Penalizing term makes initial contours flexible and simple. Level set function is initialized by a region strategy. Let  $T$  be a threshold value. The initial level set function is defined by

$$u_0(x) = \begin{cases} -t, & I(x) \geq T \\ t, & I(x) < T \end{cases} \quad (18)$$

where  $t$  is a positive constant. For the database, the parameters of DPLBF are set as  $\Delta t = 0.1$ ,  $\alpha = 0.001 \times 255 \times 255$ ,  $\beta = 1$ ,  $A_1 = A_2 = 2$ ,  $B_1 = B_2 = 1$ ,  $C_1 = C_2 = 1$ , and  $T = -400$  HU. The section images of segmented database in three axes directions (3-D coordinate system) are shown

in Fig. 5. The results of the method proposed in this paper are coherent and integrated in three axes directions. 3D surface reconstruction result of segmented database is shown in Fig. 6, in which trachea is added by a region growing segmentation algorithm. The result shows that lung texture tree is accurately extracted, and the method is much helpful for lung texture analysis and design of computer aid-diagnosis system.



(a) Lung region section images

(b) Lung texture tree section images

Fig. 5 Contrast figures of three direction sections

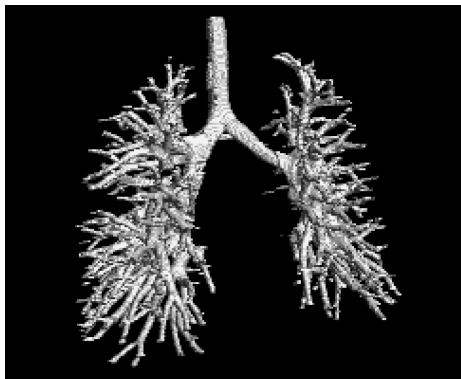


Fig. 6 Lung texture extraction results of 3D surface reconstruction

## 4 Conclusion

A novel automatic method based on LBF model is introduced to extract lung texture tree from HRCT images in this paper. An improved DPLBF model is proposed by using a dynamic parameter modulation strategy, which makes LBF model more applicable. A new technique of painting background based on nonlinear intensity transformation is used for multi-phase level set segmentation algorithm. Our method is proved to be more effective in texture extraction than region-based model and edge-based model by a number of experiments. The results of 3D database show that the method will play an important role in tree texture analysis and design of computer aid-diagnosis system.

### References

- 1 Kass M, Witkin A, Terzopoulos D. Snakes: active contour models. *International Journal of Computer Vision*, 1988, **1**(4): 321–331
- 2 Cremers D, Rousson M, Deriche R. A review of statistical approaches to level set segmentation: integrating color, texture, motion and shape. *International Journal of Computer Vision*, 2007, **72**(2): 195–215
- 3 Caselles V, Catta F, Coll T, Dibos F. A geometric method for active contours. *Numerische Mathematik*, 1993, **66**(1): 1–31
- 4 Malladi R, Sethian J A, Vemuri B C. Shape modeling with front propagation: a level set approach. *IEEE Transactions on Pattern Analysis and Machine Intelligence*, 1995, **17**(2): 158–175
- 5 Caselles V, Kimmel R, Sapiro G. Geodesic active contours. *International Journal of Computer Vision*, 1997, **22**(1): 61–79
- 6 Li C M, Xu C Y, Gui C F, Fox M D. Level set evolution without re-initialization: a new variational formulation. In: *Proceedings of IEEE Computer Society Conference on Computer Vision and Pattern Recognition*. San Diego, USA: IEEE, 2005. 430–436
- 7 Mumford D, Shah J. Optimal approximation by piecewise smooth functions and associated variational problems. *Communications on Pure and Applied Mathematics*, 1989, **42**(5): 577–685
- 8 Chan T F, Vese L A. Active contours without edges. *IEEE Transactions on Image Processing*, 2001, **10**(2): 266–277
- 9 Li C M, Kao C Y, Gore J C, Ding Z H. Implicit active contours driven by local binary fitting energy. In: *Proceedings of IEEE Conference on Computer Vision and Pattern Recognition*. Washington D. C., USA: IEEE, 2007. 1–7
- 10 Bülow T, Lorenz C, Renisch S. A general framework for tree segmentation and reconstruction from medical volume data. In: *Proceedings of the 7th International Conference on Medical Image Computing and Computer-Assisted Intervention*. Berlin, German: Springer, 2004. 533–540

- 11 Shikata H, Hoffman E A, Sonka M. Automated segmentation of pulmonary vascular tree from 3D CT images. *Proceedings of SPIE*, 2004, **5369**: 107–116
- 12 Singh H, Crawford M, Curtin J, Zwiggelaar R. Automated 3D segmentation of the lung airway tree using gain-based region growing approach. In: *Proceedings of the 7th International Conference on Medical Image Computing and Computer-Assisted Intervention*. Berlin, German: Springer, 2004. 975–982
- 13 Bulow T, Wiemker R, Blaffert T, Lorenz C, Renisch S. Automatic extraction of the pulmonary artery tree from multislice CT data. *Proceedings of SPIE*, 2005, **5746**: 730–740
- 14 Armato S G, Sensakovic W F. Automated lung segmentation for thoracic CT: impact on computer-aided diagnosis. *Academic Radiology*, 2004, **11**(9): 1011–1021
- 15 Heinemann E G. Simultaneous brightness induction as a function of inducing and test field luminances. *Journal of Experimental Psychology*, 1955, **50**(2): 89–96
- 16 Zheng Gang, Wang Hui-Nan, Li Yuan-Lu. A tree-like multiphase level set algorithm for image segmentation based on the chan-vese model. *Acta Electronics Sinica*, 2006, **34**(8): 1508–1512 (in Chinese)



**LIU Jun-Wei** Ph.D. candidate in the Department of Electronic Science and Technology, University of Science and Technology of China (USTC). He received his bachelor degree from USTC in 2004. His research interest covers image processing and analysis, level set, pattern recognition, and video compression. Corresponding author of this paper.  
E-mail: jwliu4@mail.ustc.edu.cn



**FENG Huan-Qing** Professor at the Institute of Biomedical Engineering (BME), University of Science and Technology of China (USTC). He graduated from USTC in 1970. From 1981 to 1983, he visited University of Wisconsin-Madison as a visiting scholar in the Center of BME. From 1991 to 1993, he worked as a research associate in the Department of BME, Case Western Reserve University. His research interest covers bioinformatics, medical imaging, biomedical signal processing, and computer-based medical instrumentation. E-mail: hqfeng@ustc.edu.cn



**ZHOU Ying-Yue** Master student in the Department of Electronic Science and Technology, University of Science and Technology of China. Her research interest covers medical image processing and image registration.  
E-mail: zyyzhou@mail.ustc.edu.cn



**LI Chuan-Fu** Postdoctor in the Department of Electronic Science and Technology, University of Science and Technology of China, and chief physician at the Medical Image Center, the First Affiliated Hospital, Anhui College of Traditional Chinese Medicine. His main research interest is medical imaging.  
E-mail: licf@mail.ustc.edu.cn